

Evolution with redshift of the ICM abundances

A. Martinelli¹, F. Matteucci^{1,2}, and S. Colafrancesco³

¹ Dipartimento di Astronomia, Università di Trieste, Via G.B. Tiepolo 11, 34131 Trieste, Italy

² SISSA/ISAS, Via Beirut 2–4, 34014 Trieste, Italy

³ Osservatorio Astronomico di Roma, Monte Porzio, Roma, Italy

Received 22 March 1999 / Accepted 23 July 1999

Abstract. We predict the behaviour of the abundances of α -elements and iron in the intracluster medium (ICM) as a function of redshift in poor and rich clusters. In order to do that we calculate the detailed chemical evolution of elliptical galaxies by means of one-zone and multi-zone models and then we integrate the contributions to the total gas and single elements by ellipticals over the cluster mass function at any given cosmic time which is then transformed into redshift according to the considered cosmological model.

In the case of the multi-zone model for ellipticals the more external regions evolve much faster than the internal ones which maintain a very low level of star formation almost until the present time. In other words, the outermost regions develop a galactic wind, after which the region evolves passively, at much earlier times than the innermost regions as opposed to the classic one-zone model where the galactic wind develops at early times over the whole galaxy. We refer to the one-zone model as to *burst model* and to the multi-zone model as to *continuous model*. We find that in the case of the burst model the ICM abundances should be quite constant starting from high redshifts ($z > 2$) up to now, whereas in the continuous model the ICM abundances should increase up to $z \sim 1$ and are almost constant from $z \sim 1$ up to $z = 0$.

Particular attention is devoted to the predictions of the $[\alpha/Fe]_{ICM}$ ratio in the ICM: for the burst model we predict $[\alpha/Fe]_{ICM} > 0$ over the whole range of redshifts and in particular at $z = 0$, whereas in the case of the continuous model we predict a decreasing $[\alpha/Fe]_{ICM}$ ratio with decreasing z and $[\alpha/Fe]_{ICM} \leq 0$ at $z = 0$. In particular, we predict $[O/Fe]_{ICM}(z = 0) \leq +0.35$ dex and $[Si/Fe]_{ICM}(z = 0) \leq +0.15$ dex for the burst models and $[O/Fe]_{ICM}(z = 0) \leq -0.05$ dex and $[Si/Fe]_{ICM}(z = 0) \leq +0.13$ dex for the continuous models, the precise values depending on the assumed cosmology. Finally, we discuss the influence of different cosmologies on the results.

Key words: galaxies: intergalactic medium – galaxies: evolution – galaxies: abundances

1. Introduction

The bulk of the observed X-ray emission from galaxy clusters is due to thermal bremsstrahlung in a hot gas (10^7 – 10^8 K) enriched in heavy elements. In the past two decades a great deal of attention has been devoted to the study of the abundances of heavy elements (mostly iron) in the intracluster medium. From the hot X-ray emitting intergalactic gas in clusters of galaxies a universal abundance of iron of roughly 1/3 solar has been derived (Renzini 1997 and references therein; Fukazawa et al. 1998). Attempts to explain this ICM iron abundance can be traced back to the early 1970s, when for the first time the iron-emission line in the X-ray spectra of clusters of galaxies was discovered (Mitchell et al. 1976; Serlemitsos et al. 1977). Some interpreted the presence of iron in the ICM to be due to gas ejected from galaxies, either by means of galactic winds or ram pressure stripping (Gunn & Gott 1972; Larson & Dinerstein 1975; Vigroux 1977; De Young 1978; Sarazin 1979; Himmes & Biermann 1980; Matteucci & Vettolani 1988; Renzini et al. 1993; Matteucci & Gibson 1995; Gibson & Matteucci 1997), while others suggested pregalactic objects such as population III stars as the origin (White & Rees 1978).

Recently, thanks to the results obtained with the ASCA satellite, more detailed observations of iron and α -element abundances in local galaxy clusters are becoming available. Before the launch of ASCA, spectroscopic measures of elements such as Si and S were known for the Perseus cluster (Mushotzky et al. 1981) and A576 (Rothenflug et al. 1984), indicating that the abundances of these elements as well as that of iron are roughly solar, although their level of accuracy did not allow one to make strong statements about possible differences between the α -elements and iron. Concerning oxygen there were only a few measures of the O VIII line in Virgo & Perseus (Canizares et al. 1988) indicating a higher than solar [O/Fe]. More recent measurements from ASCA by Mushotzky et al. (1996) implied $[\alpha/Fe] \approx +0.2$ – $+0.3$ dex, thus indicating a general overabundance of α -elements relative to iron in the ICM. We derived from the Mushotzky data an average $\langle (O/Fe)/(O/Fe)_{\odot} \rangle \approx 3.05 \pm 2.19$ (we estimated a formal statistical uncertainty and no systematic effect). This value corresponds (by adopting the photospheric abundances of Anders & Grevesse (1989)) to $[O/Fe] \approx +0.48^{+0.24}_{-0.55}$ dex. This means, by considering the er-

Table 1. Age (Gyr) of the elliptical galaxies for several values of the redshift z in the two cosmological models examined.

z	$\Omega_0 = 1, h = 0.5$	$\Omega_0 = 0.4, \Omega_\Lambda = 0.6, h = 0.6$
0.0	13	13
0.3	8.5	9.4
0.5	6.8	7.6
1.0	4.4	5.0
2.0	2.1	2.6
3.0	1.3	1.6
4.0	0.82	0.98
5.0	0.53	0.64

rors, a marginal (if any) overabundance of oxygen relative to iron. The average Si/Fe ratio estimated from Mushotzky data is $\langle (Si/Fe)/(Si/Fe)_\odot \rangle \approx 2.32 \pm 1.30$ corresponding to $[Si/Fe] = +0.37^{+0.17}_{-0.35}$ dex, which agrees with the same ratio obtained by Fukazawa et al. (1998) in their analysis of about 40 nearby poor and rich clusters. In fact, from this latter compilation of data we derived $\langle (Si/Fe)/(Si/Fe)_\odot \rangle \approx 3.15 \pm 1.60$ for clusters with $T > 3$ keV (we consider these clusters as rich according to our definition in Table 2) and $\langle (Si/Fe)/(Si/Fe)_\odot \rangle \approx 1.39 \pm 0.90$ for clusters with $T \leq 3$ keV (poor clusters).

Ishimaru & Arimoto (1997a,b) and Arimoto et al. (1997) claimed that the present uncertainties both on the assumed solar abundances (used to derive the quantity $[O/Fe]$) and on the derived X-ray abundances are consistent with almost solar values of the $[\alpha/Fe]$ ratios in the ICM. In particular, the use of the meteoritic abundances for the sun (Anders & Grevesse 1989) instead of the photospheric ones used in the previous studies, would reduce the $[\alpha/Fe]$ values quoted above by ≈ 0.16 dex (Ishimaru & Arimoto 1997a,b; Renzini 1997).

Therefore, we consider all of these observational results still preliminary and subject to variation.

Concerning the evolution of the abundances and abundance ratios as a function of redshift very little is known at the moment. However, preliminary results by Mushotzky & Lowenstein (1997) seem to indicate no evolution in the Fe abundance for $z \simeq 0.5$.

In this paper we study the chemical evolution of the ICM, in particular we predict the evolution of Fe and $[\alpha/Fe]$ ratios as functions of redshift. This is because the value of the $[\alpha/Fe]$ ratio as well as the Fe abundance in the ICM impose strong constraints on the evolution of the galaxies in clusters as well as on the roles of supernovae of different types in the enrichment of the ICM, as discussed by Renzini et al. (1993) and Matteucci & Gibson (1995).

Since the heavy elements in the ICM are likely to come from ellipticals, as shown by Arnaud (1994), it is important to explore different kinds of models for the evolution of ellipticals. In particular, we will use either a one-zone model (Matteucci & Gibson 1995, hereafter referred to as “burst model”) and a multi-zone model (Martinelli et al. 1998, hereafter “continuous model”) for elliptical galaxies. The continuous model, which predicts abundance gradients in ellipticals in very good agree-

Table 2. Input ingredients for rich and poor cluster models.

Cluster	α	f	n_*	M_*
RC	-1.3	0.8	115	-22.5
PC	-1.3	0.3	20	-22.0

ment with the observed ones, assumes that the outermost regions of these galaxies experience early galactic winds whereas the innermost ones keep an active, although low, star formation rate until late times. The physical reason for this resides in the fact that the binding energy of the gas is lower in the outermost galactic regions and this is supported by the observational finding of a correlation between metallicity and escape velocity in ellipticals (Carollo & Danziger, 1994). The late occurrence of galactic winds in the most internal regions of ellipticals, if true, has an effect on the chemical evolution of the ICM, certainly at variance with the predictions by models with only early winds (Matteucci & Gibson 1995; Gibson & Matteucci, 1997).

The plan of this paper is the following. In Sect. 2 we present the models and the computational method. In Sect. 3 the results are discussed and some conclusions are drawn. We use throughout the paper an adimensional Hubble parameter $h = H_0/(100 \text{ km s}^{-1} \text{ Mpc}^{-1})$.

2. Computational method of the heavy element abundances in galaxy clusters

The mass in the form of specific chemical elements as well as the total gas masses ejected by the elliptical galaxies both at early and late galactic lifetimes into the ICM, can be computed in detail once a chemical evolution model is assumed.

Two different models for the evolution of elliptical galaxies have been taken into account:

1. *burst models*, namely those with only one major episode of galactic wind which occurs simultaneously all over the galaxy;
2. *continuous models*, where the galactic wind starts at an early epoch in the most external regions of the galaxies and continues until the present time in the most internal ones.

The burst model is the same as in Matteucci & Gibson (1995), where we direct the reader for details, in the case of the Arimoto & Yoshii (1987) IMF. This is their best model and we refer to it as CWM.

The continuous wind model is described in Martinelli et al. (1998), where we direct the reader for details. The basic difference of this approach, relative to the model of Matteucci & Gibson (1995), is that the elliptical galaxy is divided in several shells not interacting. For each shell the potential energy of the gas is calculated and compared with the thermal energy of the gas due to supernova explosions. A galactic wind develops first in the outermost shells and then progressively in the inner ones. An improved expression for the cooling time of SN (of both types) remnants as well as a detailed description of the potential energy of the gas are used in this model. The

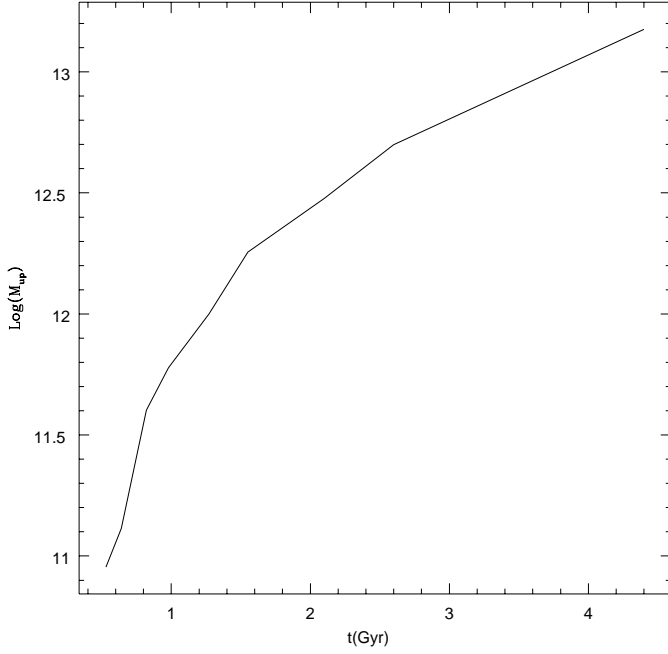


Fig. 1. Mass $M_{up}(t)$ (in solar masses) of the most massive galaxy which develops a galactic wind at the time t , in the case of the burst model.

SN remnant cooling time strongly influences the occurrence of a galactic wind as well as the amount of energy that SNe can transfer into the interstellar medium (ISM). In the CWM model, a cooling time not dependent on time was used, whereas in the continuous models the cooling time depends on the gas density ($t_c \sim \frac{1}{\sqrt{\rho_{gas}}}$) which is a function of time.

In both models, after the occurrence of a galactic wind it is assumed that star formation is no longer taking place, and the galaxy or the galactic region evolves passively after that. In the case of the continuous model, the innermost regions (inside 30 pc) never develop a galactic wind and the star formation continues until late times although it is so low that it would be hardly detectable. In the outer shells, once the wind is established in a given shell, it continues until the shell is devoided of gas. This is because the gas restored by dying stars is suddenly heated by the energy released by SNe Ia, which continue to explode even after star formation has stopped.

The chemical evolution of the ICM is caused by two different processes:

1. In the burst model, galaxies begin to eject the gas only after the time of occurrence of a galactic wind (t_{GW}), and this process lasts only for few 10^8 years. The time t_{GW} is a function of the initial galactic mass which influences the potential well. Therefore, when the time of the first occurrence of the galactic wind increases, namely when more and more massive galaxies achieve the conditions to develop a wind, the number of galaxies contributing to the enrichment of the ICM also increases, as shown in Fig. 1. This type of evolution stops at the time $t_{GWM_{ax}}$, corresponding to the

onset of the galactic wind for the galaxy with the highest mass considered.

2. In the continuous models, the ICM evolution is caused by the gas ejected continuously by each galaxy after the time t_{GW} . This continuous ejection process, not present in the burst models, has the characteristic of acting also at low redshift. The assumed IMF is the same as in the burst model.

2.1. Stellar yields in both models

We assumed that type II SNe originate from explosions of single massive stars ($M \geq 10M_{\odot}$) and assumed the yields of Woosley & Weaver (1995) for the production of the α -elements and Fe. In particular we adopted the same yields which best reproduce the solar neighbourhood constraints (Chiappini et al. 1997) and correspond to case B of Woosley & Weaver (1995). The progenitors of SNe Ia are assumed to be C-O white dwarfs in binary systems accreting material from a companion and exploding when the Chandrasekhar mass is reached. The computation of the SNIa rate follows the prescriptions of Matteucci & Greggio (1986). The masses of the progenitors of both the primary (the white dwarf) and secondary star in the binary system are in the range $0.8-8M_{\odot}$. The yields from SN Ia are taken from Nomoto et al. (1984) and Thielemann et al. (1993). These supernovae contribute mostly to Fe and to a certain extent to Si but negligibly to all the other elements.

Finally for single low and intermediate mass stars, again in the range $0.8-8M_{\odot}$ we adopted the yields of Renzini & Voli (1981). These stars produce mostly 4He , C and N.

2.2. Dark matter halos in both models

We adopted in both models the same prescription for the dark matter distribution, namely that one described by Bertin et al. (1992):

$$M_{Dark}(r) = \frac{2M_{Dark}}{\pi} \left[\arctg(r/r_0) - \frac{r/r_0}{1 + (r/r_0)^2} \right] \quad (1)$$

with $r_0 = 0.45R_{Dark}$. In both cases we assume that the ratio between dark and luminous mass is 10 and the ratio between the effective radius of luminous matter and the radius of dark matter is $r_L/r_D = 0.1$ for all galaxies.

We compute the binding energy of the gas as the energy necessary to carry the gas out of the galaxy. In the burst models we define the binding energy of the gas as:

$$E_{Bgas} = \int_0^{\infty} dL(r) \quad (2)$$

where $dL(r)$ is the energy required to carry out a quantity $dm = 4\pi r^2 \rho_{gas}(r, t) dr$ of gas. Therefore, we have for $dL(r)$:

$$dL(r) = \int_r^{\infty} dr' f(r') \quad (3)$$

where $f(r')$ is the force between dm and the total mass (dark and luminous) within r' which reads as:

$$f(r') = \frac{GM(r')dm}{r'^2} \quad (4)$$

The total mass at radius r' , $M(r')$, is given by:

$$M(r') = M_{Dark}(r') + M_{Lum}(r') \quad (5)$$

where the luminous mass can be written as the sum of the gaseous and stellar components:

$$M_{Lum}(r') = M_{gas}(r') + M_*(r') \quad (6)$$

In the case of continuous models for each shell with thickness ΔR_i and internal and external radii R_i and $R_{i+1} = R_i + \Delta R_i$ respectively, the energy E_{Bgas} can be written as follows:

$$E_{Bgas}^i = \int_{R_i}^{R_i + \Delta R_i} dL(r) \quad (7)$$

where $dL(r)$ is

$$dL(r) = \int_r^{1.5R_L} dr' f(r') \quad (8)$$

i.e. the removal of material from each galactic region was intended now just beyond the effective radius (at variance with the burst model where the integral is extended up to infinite).

We now elucidate, in some detail, how we have calculated the chemical abundances in the ICM for several values of redshift, according to the two elliptical galaxy models described above.

2.3. Burst models

We computed the ejected masses of each element (Fe, Si, O, and total gas) as functions of several initial galactic masses (the procedure we describe here can be also found in Matteucci & Vettolani, 1988). We found that the relation between the generic chemical element i and the initial galactic mass can be approximated by a power law:

$$M_i = E_i M_G^{\beta_i} \quad (9)$$

where M_i represents the mass ejected in the form of the chemical species i by a galaxy of initial mass M_G , and E_i and β_i are two constants (that can be fixed by a least squares fit). We have normalized the relations (9) to a galaxy at the *break* of the luminosity function of a cluster (Schechter 1976) having a blue luminosity L_* , absolute blue magnitude M_* and total mass M_{G_*} .

In particular:

$$\frac{M_i}{M_{i_*}} = \left(\frac{M_G}{M_{G_*}} \right)^{\beta_i} = \left(\frac{L}{L_*} \right)^{\beta_i} \quad (10)$$

where M_{i_*} represents the mass ejected in the form of an element i by the galaxy with mass M_{G_*} .

For each redshift z we evaluated, for the cosmological model considered, the corresponding age t of the elliptical galaxies (Table 1). Then, for each t we determined from Fig. 1 the mass $M_{up}(t)$ of the most massive galaxy which develops a galactic wind just at the time t . The maximum mass considered is $M_{up}(t) = M_{up} = 2 \cdot 10^{12} M_\odot$. Let M_{low} ($10^8 M_\odot$) be the

smallest mass for elliptical galaxies in our models. It is worth noting that the lower limit for the galactic mass does not have much influence on the results, since the critical mass is the mass at the break of the luminosity function, as discussed by Matteucci & Vettolani (1988).

Let finally $L_{up}(t)$ and L_{low} be the luminosities related to the previous mass bounds. Therefore, by integrating over all the galaxies with luminosity between L_{low} and $L_{up}(t)$, we show that the total mass in the form of an element i , ejected into the ICM is:

$$M_i^T = \int_{L_{low}}^{L_{up}(t)} \Phi(L/L_*) (L/L_*)^{\beta_i} d(L/L_*) \quad (11)$$

where $\Phi(L/L_*) (L/L_*)^{\beta_i} d(L/L_*)$ represents the mass of an element i per interval of $d(L/L_*)$. The masses computed by Eq. (11) are therefore expressed in units of an element i ejected by a galaxy of luminosity L_* , namely of mass M_{G_*} (the luminosity and the mass at the break of the luminosity function). The luminosity function $\Phi(L/L_*)$ is taken to be Schechter (1976), namely:

$$\Phi(L/L_*) = n^* (L/L_*)^\alpha \exp(-L/L_*) \quad (12)$$

where n^* is a measure of the cluster richness and $\alpha = 1.3$.

Integrating the previous Eq. (11) one obtains:

$$M_i^T = n^* f[\Gamma(\alpha + 1 + \beta_i, L_{low}/L_*) - \Gamma(\alpha + 1 + \beta_i, L_{up}(t)/L_*)] \quad (13)$$

where $\Gamma(a, b)$ is the incomplete Γ function and f represents the fraction by number of ellipticals in a cluster. The parameters f , n^* , α and M_* are fixed for each individual cluster. We consider here the evolution of the ICM chemical abundances for two galactic systems: a rich cluster (RC) and a poor cluster (PC). In Table 2 the values of the parameters related to these prototype clusters are given.

At this point we need to express Eq. (13) as a function of the galactic mass instead of the luminosity. We obtain:

$$M_i^T = E_i n^* f (h^2 K)^{\beta_i} 10^{-0.4\beta_i(M_* - 5.48)} [\Gamma(\alpha + 1 + \beta_i, (M_{low} h^2 / K) 10^{-0.4(M_* - 5.48)}) - \Gamma(\alpha + 1 + \beta_i, (M_{up}(t) h^2 / K) 10^{-0.4(M_* - 5.48)})] \quad (14)$$

where $K = M_G/L$ is the mass to luminosity ratio, with M_G expressed in solar masses and L in solar luminosities, $h^{-1} = H_0/100$ with H_0 the Hubble constant. The mass to luminosity ratio is computed as a function of the assumed IMF, as described in Matteucci & Gibson (1995).

2.4. Continuous models

In the case of continuous models the computation is different from the previous case because now the quantities E_i and β_i are time dependent. For each value of t we calculate the mass of gas in the form of a specific chemical element ejected from each galaxy. Again we can find the corresponding values of $E_i(t)$ and $\beta_i(t)$ by using a least squares fit. By substituting these quantities

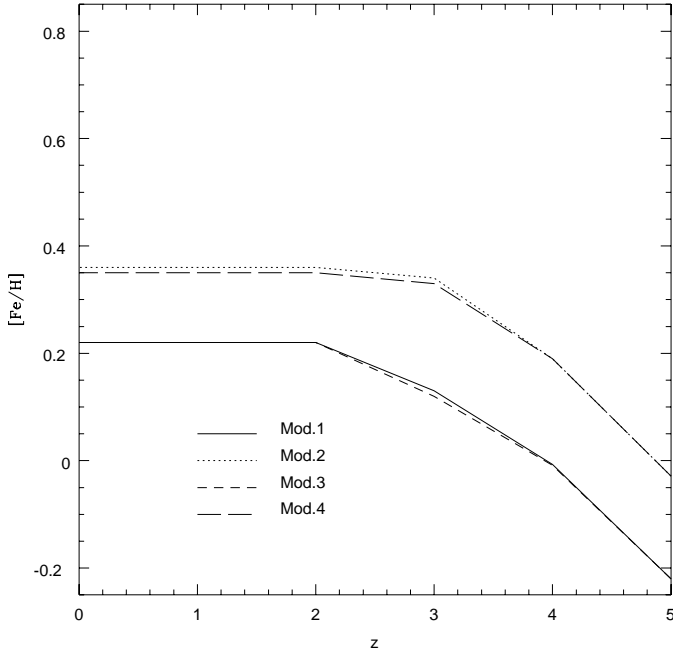


Fig. 2. $[\frac{Fe}{H}] = \log(Fe/H) - \log(Fe/H)_{\odot}$ in the total gas ejected from the ellipticals as a function of the redshift in the case of burst models. The curves refer to a poor and a rich clusters and to different cosmologies as shown in Table 3. The adopted solar abundances are the meteoritic abundances from Anders & Grevesse (1989).

Table 3. Models considered.

Mod.	Cluster	Cosmology
1	RC	$\Omega_0 = 1, h = 0.5$
2	RC	$\Omega_0 = 0.4, \Omega_{\Lambda} = 0.6, h = 0.6$
3	PC	$\Omega_0 = 1, h = 0.5$
4	PC	$\Omega_0 = 0.4, \Omega_{\Lambda} = 0.6, h = 0.6$

in Eq. (14) we then can calculate the total mass of the chemical element i ejected into the ICM at the time t .

The evolution of the elliptical galaxies is considered in the framework of different cosmological models: a flat, scale invariant CDM cosmology with $\Omega_0 = 1, h = 0.5$ and a vacuum dominated CDM model with $\Omega_0 = 0.4, \Omega_{\Lambda} = 0.6$ and $h = 0.6$.

In all the models considered we set the galaxy formation epoch, $z_{GF} = 10$, and their age = 13 Gyr (we consider the same age for all the galaxies in our code).

The models are defined in Table 3.

3. Results and conclusions

In this paper we have computed the evolution of the abundances of Fe and α -elements in the ICM of poor and rich clusters as a function of redshift under different cosmologies. To do that we have used two different models for the chemical evolution of elliptical galaxies, which are the main contributors to the ICM enrichment. In particular, we used a model where the galactic wind develops at the same time all over the galaxy (the burst model) and after that the galaxy evolves only passively not contributing

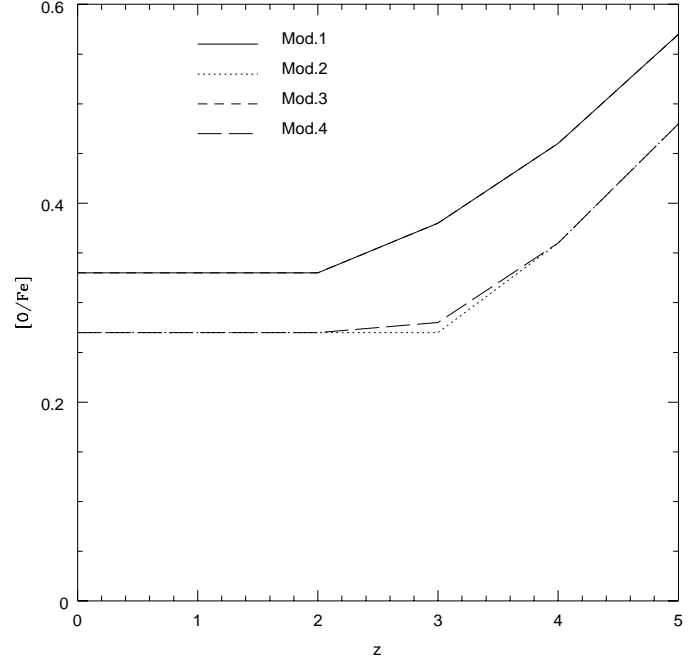


Fig. 3. $[\frac{O}{Fe}]$ in the total gas ejected from ellipticals and in the ICM as a function of the redshift in the case of burst models. The curves refer to a poor and a rich cluster and different cosmologies as shown in Table 3.

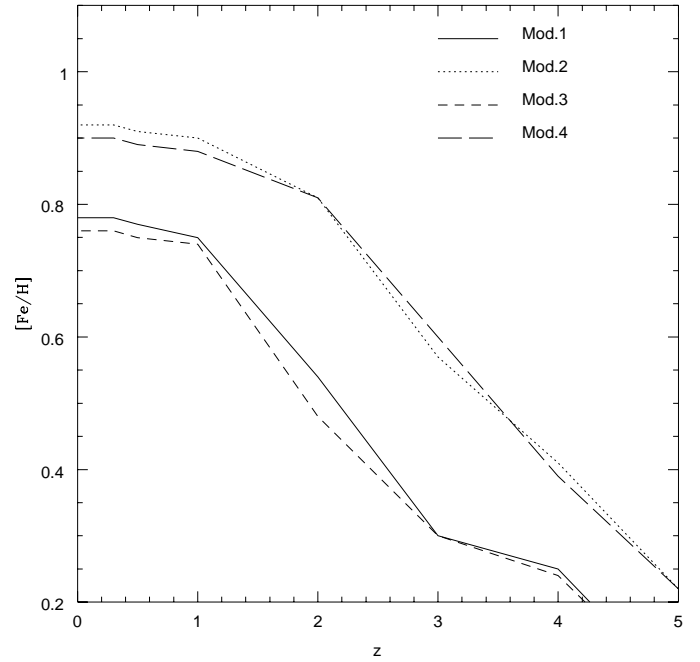


Fig. 4. $[\frac{Fe}{H}]$ in the total gas ejected from ellipticals as a function of the redshift in the case of continuous models.

any longer to the ICM enrichment, and a model where galactic winds develop first at large galactocentric distances and then progressively later in the innermost zones (continuous model).

Our results are shown in Figs. 2–9, where the behaviour of the $[\frac{Fe}{H}]$, $[\frac{O}{Fe}]$ and $[\frac{Si}{Fe}]$ as functions of the redshift z in the cases of burst models (Figs. 2, 3, 6, 8) and continuous models (Figs. 4, 5, 7, 9) is indicated. It should be noted that the $[Fe/H]$

and the $[\alpha/\text{Fe}]$ abundances refer to the abundances expected in the total gas ejected by ellipticals and not mixed with the pristine gas in the cluster. Previous calculations (Matteucci & Vettolani, 1988; Matteucci & Gibson, 1995; Gibson & Matteucci 1997) have shown that while the predicted total iron mass ejected by ellipticals agrees with the observed iron mass in clusters the total mass of gas ejected from ellipticals is much lower than the observed total gas mass in clusters. This is interpreted as due to the fact that most of the gas in clusters should be pristine gas.

The models presented here also predict a too small amount of ejected total gas as compared to the observed one. A larger production of total gas from galaxies can be obtained by adopting a steep faint end slope of the luminosity function. However, Gibson & Matteucci (1997) showed that in this case the contribution of the dwarf ellipticals is at most 15% of the total ICM gas, so that the conclusion about most of the ICM gas being pristine gas remains unaffected. In order to obtain the abundances in the ICM we should rescale the abundances shown in Figs. 2 and 4 to the total observed mass of gas in a typical poor and a rich cluster by assuming that most of it is pristine gas. In order to compute the evolution of the abundances as a function of redshift we also assumed that the amount of pristine gas in the clusters did not change during the cluster lifetime, in agreement with the results of White et al. (1993) which found that the baryon fraction in clusters should have been constant.

After doing that, by taking $M_{gasICM_R} = 4.4 \cdot 10^{14} M_\odot$ as representative of the total gas of a rich cluster (Coma) and $M_{gasICM_P} = 2 \cdot 10^{13} M_\odot$ as representative of a poor cluster (Virgo) we found that, in order to represent the $[Fe/H]_{ICM}$, the curves of Fig. 2 should be lowered by -1.48 and -1.35 dex for a rich and a poor cluster, respectively, whereas the curves of Fig. 4 should be lowered by -1.37 and -1.30 for a rich and a poor cluster, respectively. The present time iron abundance, Fe_{ICM} , obtained in this way from the continuous models is in very good agreement with the observational estimates of the iron abundance in local clusters. In fact, the continuous models predict $Fe_{ICM}(z=0) \sim 0.3Fe_\odot$ both for poor and rich clusters, whereas the burst models predict a lower abundance ($Fe_{ICM}(z=0) \sim 0.1Fe_\odot$).

On the other hand, the abundance ratios $[\alpha/\text{Fe}]$ are completely unaffected by the amount of gas in the clusters and therefore the abundance ratios in the gas ejected from ellipticals represent also the abundance ratios in the ICM. For this reason we want to stress the importance of considering abundance ratios rather than absolute abundances.

From Figs. 2–9 we can infer the following conclusions:

- We observe that in the burst models the chemical evolution of the ICM stops entirely at $z = 3$ when the cosmological parameters are $\Omega_0 = 0.4$, $\Omega_\Lambda = 0.6$, $h = 0.6$ and at $z = 2$ when $\Omega_0 = 1$, $\Omega_\Lambda = 0.0$ and $h = 0.5$, respectively.
- In the case of continuous models there is a continuous evolution up to $z \simeq 1$ and negligible evolution from $z \simeq 1$ up to $z = 0$.
- The predicted $[\text{Fe}/\text{H}]$ at the present time in the ICM is in very good agreement with the observations (1/3 solar) for

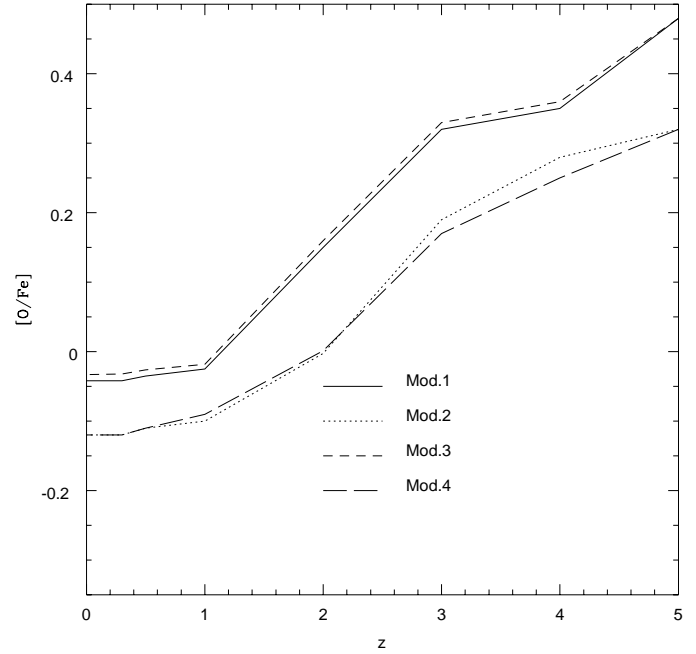


Fig. 5. $[\frac{O}{Fe}]$ in the total gas ejected from ellipticals and in the ICM as a function of the redshift in the case of continuous models

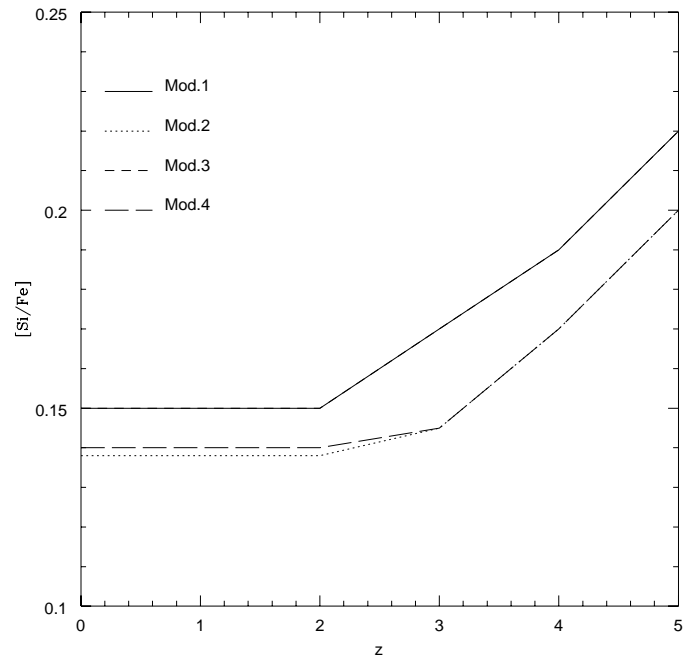


Fig. 6. $[\frac{Sr}{Fe}]$ in the total gas ejected from ellipticals and in the ICM as a function of the redshift in the case of burst models. The curves refer to a poor and a rich cluster and different cosmologies as shown in Table 3.

the continuous models whereas the burst models predict a lower abundance.

- For the $[\alpha/Fe]_{ICM}$ ratios we predict $[\alpha/Fe]_{ICM} > 0$ at $z = 0$ in the burst models and $[\alpha/Fe]_{ICM} \leq 0$ at $z = 0$ for the continuous models, the exact values of the $[\alpha/Fe]_{ICM}$ ratio depending on the assumed cosmology. In particular, at $z = 0$ we predict $[O/Fe]_{ICM} \simeq +0.27 \div +0.37$ dex and

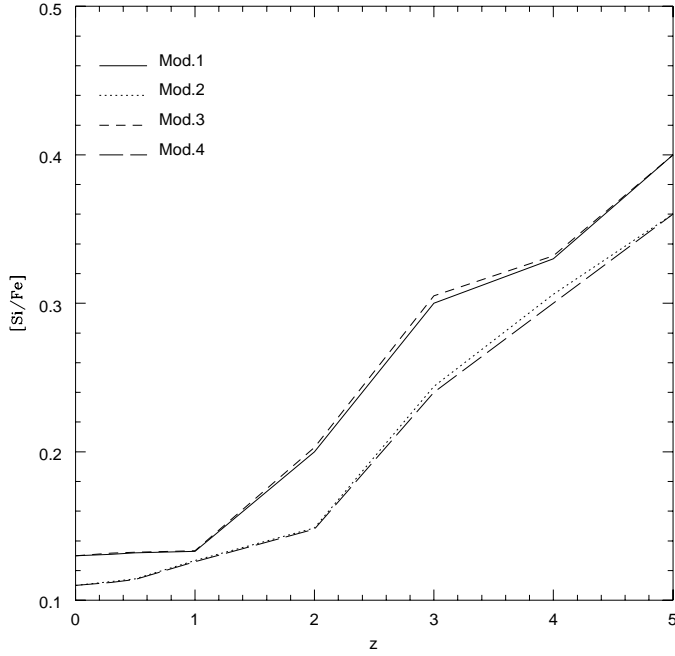


Fig. 7. $[Si/Fe]$ in the total gas ejected from ellipticals and in the ICM as a function of the redshift in the case of burst models. The curves refer to a poor and a rich cluster and different cosmologies as shown in Table 3.

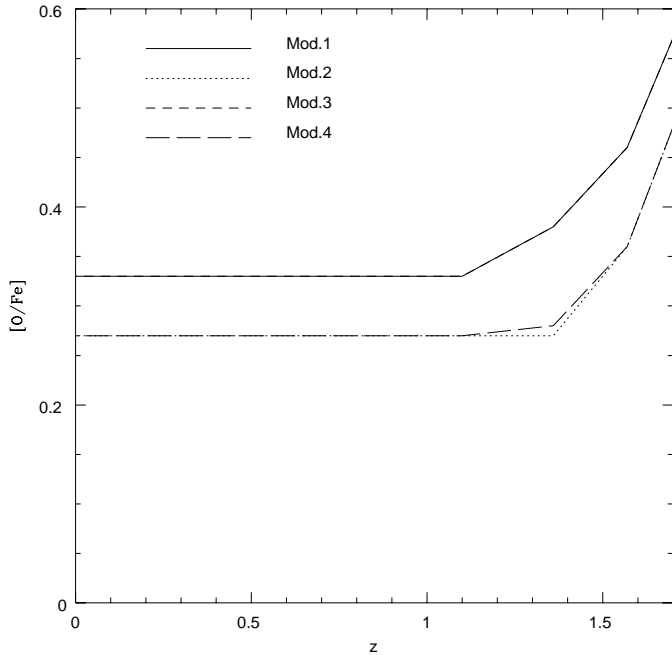


Fig. 8. The same as Fig. 3 but for a galaxy formation redshift $z_{GF} = 2$ instead of $z_{GF} = 10$.

$[Si/Fe]_{ICM} \simeq +0.14 \div +0.15$ dex for the bursts models and $[O/Fe]_{ICM} \simeq -0.12 \div -0.05$ dex and $[Si/Fe]_{ICM} \simeq +0.11 \div +0.13$ dex for the continuous models. These values were derived by adopting the meteoritic solar abundances (Anders & Grevesse, 1989).

In both cases (different normalization to the solar abundances) the predicted $[\alpha/Fe]_{ICM}$ ratios at the present time

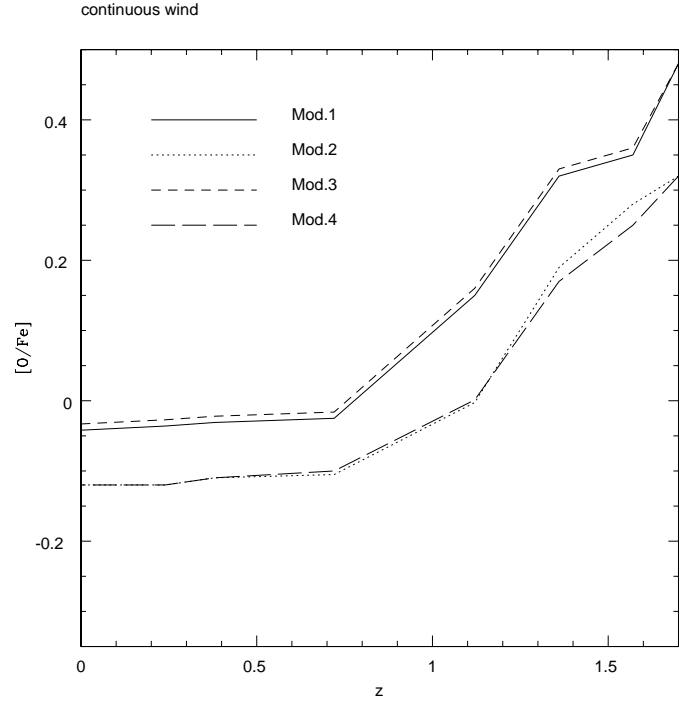


Fig. 9. The same as Fig. 5 but for a galaxy formation redshift $z_{GF} = 2$ instead of $z_{GF} = 10$.

are higher in the burst than in the continuous model. The main reason for this behaviour of the $[\alpha/Fe]_{ICM}$ ratio in the two different cases is the fact that in the burst model the galactic wind develops at early times in all galaxies and therefore it is mainly enriched by the products of SNe II (high $[\alpha/Fe]$ ratio). On the other hand, in the continuous model the galactic wind continues to develop until the present time and therefore it is enriched also by the products of SNe Ia (low $[\alpha/Fe]$ ratio). This result is quite important since it depends uniquely on the evolution of the ellipticals and not on the particular history of the cluster evolution (infall, etc..) as it is for absolute abundances. We note that the predicted present time $[Si/Fe]_{ICM}$ ratios are larger than the present time $[O/Fe]_{ICM}$ for the continuous models. This is due to the different nucleosynthesis of Si and O: O, in fact, is entirely produced by SNe II whereas Si is mostly produced by SNe II but a fraction, not entirely negligible, arises from SNe Ia and this contributes to avoid that the Si/Fe ratio decreases too much, since the bulk of Fe coming from SNe Ia is partly compensated by the Si which comes also from SNe Ia. For this reason Si is not the best α -element to be used to check the $[\alpha/Fe]$ ratio, whereas Mg and O should be preferred.

Finally, it is worth noting that these $[\alpha/Fe]_{ICM}$ ratios have been obtained by adopting a flat IMF in the galactic models ($x = 0.95$). These values are therefore upper values especially in the case of the continuous model, since the adoption of the Salpeter IMF ($x = 1.35$) would lead to lower present time values of these ratios, due to the larger contribution from type Ia SNe relative to type II SNe.

- For both galactic models these results do not differ for rich or poor clusters.
- The effect of a change in the cosmological parameters is a simple translation of the abundance ratios (namely the $[\alpha/Fe]$ ratios are lower by at most ~ 0.1 dex when $\Omega_0 = 0.4$ than when $\Omega_0 = 1$). A change in the cosmology produces also a delay in the chemical evolution, in the sense that when $\Omega_0 = 1$ the chemical evolution of the ICM stops a little later than when $\Omega_0 = 0.4$. This is a consequence of the different correspondence between the redshift z and the galactic age t as shown in Table 1.

The redshift of galaxy formation in all models has been assumed to be $z_{GF} = 10$. However, if we assume a lower redshift, such as $z_{GF} = 2.0$, the main results concerning abundances and abundance ratios at the present time are unchanged.

However, the curves representing the evolution of the abundance ratios contract and shift, as shown in Figs. 8 and 9.

From the previous results we can conclude that if we want to see an evolution in the ICM we have to be able to perform observations of abundances in very high redshift clusters (at least $z \geq 1$). Preliminary results from ASCA (Mushotzky & Lowenstein, 1997) seem to indicate no evolution in the abundance of Fe for $z \leq 0.5$ in agreement with our results related to all models here considered. Therefore, on this basis alone we cannot distinguish among the two models. Concerning our predictions on the $[\alpha/Fe]_{ICM}$ ratios, recent studies (Ishimaru & Arimoto, 1997a,b) adopting the meteoritic solar abundances of Anders & Grevesse (1989) as in this work, seem to favor a low value of this ratio in very good agreement with our continuous wind model predictions.

Acknowledgements. A. M. would like to thank SISSA for the kind hospitality during the development of this work.

References

- Anders E., Grevesse N., 1989, *Geochim. Cosmochim. Acta* 53, 197
 Arimoto N., Yoshi Y., 1987, *A&A* 173, 23
 Arimoto N., Matsushita K., Ishimaru Y., Ohashi T., Renzini A., 1997, *ApJ* 477, 128
 Arnaud M., 1994, In: Durret F., et al. (eds.) *Clusters of Galaxies. Editions Frontieres, Gif-sur-Yvette*, p. 211
 Bertin G., Saglia R.P., Stiavelli M., 1992, *ApJ* 384, 423
 Canizares C.R., Markert T.H., Donahue M.E., 1988, In: Fabian A.C. (eds.) *Cooling Flows in Clusters and Galaxies. Kluwer, Dordrecht*, p. 63
 Carollo M., Danziger I.J., 1994, *MNRAS* 270, 523
 Chiappini C., Matteucci F., Gratton R., 1997, *ApJ* 477, 765
 De Young D.S., 1978, *ApJ* 223, 47
 Fukazawa Y., Makishima K., Tamura T., et al., 1998, *PASJ* 50, 187
 Gibson B.K., Matteucci F., 1997, *ApJ* 475, 47
 Gunn J.E., Gott J.R., 1972, *ApJ* 176, 1
 Himmes A., Biermann P., 1980, *A&A* 86, 11
 Ishimaru Y., Arimoto N., 1997a, *PASJ* 49, 11
 Ishimaru Y., Arimoto N., 1997b, *IAUS* 187, *Cosmic Chemical Evolution. Kyoto, Japan*
 Larson R.B., Dinerstein H.L., 1975, *PASP* 87, 911
 Martinelli A., Matteucci F., Colafrancesco S., 1998, *MNRAS* 298, 42
 Matteucci F., Greggio L., 1986, *A&A* 154, 279
 Matteucci F., Vettolani G., 1988, *A&A* 202, 21
 Matteucci F., Gibson B., 1995, *A&A* 304, 11
 Mitchell R.J., Culhane J.L., Davison P.J.N., Ives J.C., 1976, *MNRAS* 176, 29
 Mushotzky R.F., Holt S.S., Smith B.W., Boldt E.A., 1981, *ApJ* 225, 21
 Mushotzky R.F., Loewenstein M., Arnaud M., et al., 1996, *ApJ* 466, 686
 Mushotzky R.F., Loewenstein M., 1997, *ApJ* 481, L63
 Nomoto K., Thielemann F.K., Yokoi K., 1984, *ApJ* 286, 644
 Renzini A., Ciotti L., D'Ercole A., Pellegrini S., 1993, *ApJ* 419, 52
 Renzini A., 1997, *ApJ* 488, 35
 Renzini A., Voli M., 1981, *A&A* 94, 175
 Rothenflug R., Vigroux L., Mushotzky R.F., Holt S.S., 1984, *ApJ* 279, 53
 Schechter P., 1976, *ApJ* 203, 297
 Selermitsos P.J., Smith B.W., Boldt E.A., Holt S.S., Swank J.H., 1977, *ApJ* 211, L63
 Sarazin C.L., 1979, *Astrophys. Lett.* 20, 93
 Thielemann F.K., Nomoto K., Hashimoto M., 1993, In: Prantzos N., et al. (eds.) *Origin and Evolution of the Elements. Cambridge Univ. Press*, p. 297
 Vigroux L., 1977, *A&A* 56, 473
 White S.D.M., Rees M.J., 1978, *MNRAS* 183, 341
 White S.D.M., Navarro J.F., Evrard A.E., Frenk C.S., 1993, *Nat* 366, 429
 Woosley S.E., Weaver T.A., 1995, *ApJS* 101, 181